JVI Journals.ASM.org

Particle-to-PFU Ratio of Ebola Virus Influences Disease Course and Survival in Cynomolgus Macaques

Kendra J. Alfson,[a,b] Laura E. Avena,[a] Michael W. Beadles,[a*] Hilary Staples,[a] Jerritt W. Nunneley,[a*] Anysha Ticer,[a] Edward J. Dick, Jr.,[c] Michael A. Owston,[c] Christopher Reed,[d*] Jean L. Patterson,[a] Ricardo Carrion, Jr.,[a] Anthony Griffiths[a,b]

Department of Virology and Immunology, Texas Biomedical Research Institute, San Antonio, Texas, USA[a]; Department of Microbiology and Immunology, University of Texas Health Science Center at San Antonio, San Antonio, Texas, USA[b]; Southwest National Primate Research Center, Texas Biomedical Research Institute, San Antonio, Texas, USA[c]; Division of Virology, U.S. Army Medical Research Institute of Infectious Diseases, Frederick, Maryland, USA[d]

ABSTRACT

This study addresses the role of Ebola virus (EBOV) specific infectivity in virulence. Filoviruses are highly lethal, enveloped, single-stranded negative-sense RNA viruses that can cause hemorrhagic fever. No approved vaccines or therapies exist for filovirus infections, and infectious virus must be handled in maximum containment. Efficacy testing of countermeasures, in addition to investigations of pathogenicity and immune response, often requires a well-characterized animal model. For EBOV, an obstacle in performing accurate disease modeling is a poor understanding of what constitutes an infectious dose in animal models. One well-recognized consequence of viral passage in cell culture is a change in specific infectivity, often measured as a particle-to-PFU ratio. Here, we report that serial passages of EBOV in cell culture resulted in a decrease in particle-to-PFU ratio. Notably, this correlated with decreased potency in a lethal cynomolgus macaque (*Macaca fascicularis*) model of infection; animals were infected with the same viral dose as determined by plaque assay, but animals that received more virus particles exhibited increased disease. This suggests that some particles are unable to form a plaque in a cell culture assay but are able to result in lethal disease *in vivo*. These results have a significant impact on how future studies are designed to model EBOV disease and test countermeasures.

IMPORTANCE

Ebola virus (EBOV) can cause severe hemorrhagic disease with a high case-fatality rate, and there are no approved vaccines or therapies. Specific infectivity can be considered the total number of viral particles per PFU, and its impact on disease is poorly understood. In stocks of most mammalian viruses, there are particles that are unable to complete an infectious cycle or unable to cause cell pathology in cultured cells. We asked if these particles cause disease in nonhuman primates by infecting monkeys with equal infectious doses of genetically identical stocks possessing either high or low specific infectivities. Interestingly, some particles that did not yield plaques in cell culture assays were able to result in lethal disease *in vivo*. Furthermore, the number of PFU needed to induce lethal disease in animals was very low. Our results have a significant impact on how future studies are designed to model EBOV disease and test countermeasures.

Ebola virus (EBOV) is a filovirus that can cause hemorrhagic fever with high case-fatality rates (1). Filoviruses can replicate in many hosts, including humans, nonhuman primates (NHPs), and pigs (2, 3). Filoviruses also show great potential for emergence: in new geographic regions, in new hosts, and by new modes of transmission (3–6). No approved vaccines or therapies exist for filovirus infections, and the West African outbreak that became the largest Ebola virus disease (EVD) outbreak on record, in 2014, highlights the urgency for advancements in this area (7).

As efficacy testing of new countermeasures in humans is not ethical, any studies aimed at developing countermeasures against filovirus infections may be subject to the U.S. Food and Drug Administration's Animal Efficacy Rule (8, 9). This rule permits the substitution of animals for humans in efficacy trials of countermeasures against highly lethal pathogens (10, 11). Consequently, the development and testing of effective countermeasures against EBOV require excellent animal models and a thorough understanding of those models (11, 12). Furthermore, the unprecedented West African outbreak has led public health officials and scientists to recognize the critical importance of understanding more about EBOV. Further information about certain viral properties and how they relate to human infection can help guide public health officials and medical interventions (13).

Specific infectivity can be described as the number of viral particles present for every one particle that is able to infect a cell in culture. This is often represented as the ratio of particles per PFU; a lower ratio means that more of the viral particles yield plaques in

Received 10 March 2015 **Accepted** 8 April 2015

Accepted manuscript posted online 22 April 2015

Citation Alfson KJ, Avena LE, Beadles MW, Staples H, Nunneley JW, Ticer A, Dick EJ, Jr, Owston MA, Reed C, Patterson JL, Carrion R, Jr, Griffiths A. 2015. Particle-to-PFU ratio of Ebola virus influences disease course and survival in cynomolgus macaques. J Virol 89:6773–6781. doi:10.1128/JVI.00649-15.

Editor: T. S. Dermody

Address correspondence to Anthony Griffiths, agriffiths@txbiomed.org.

* Present address: Michael W. Beadles, Bexar County Medical Examiner's Office, San Antonio,Texas, USA; Jerritt W. Nunneley, ENV Services, Inc., Hatfield, Pennsylvania,USA; Christopher Reed, Virginia Tech Carilion School of Medicine, Roanoke, Virginia, USA.

doi:10.1128/JVI.00649-15

the cell culture system tested (14, 15). Viral particle/PFU ratios are dependent on both the virus and assay system (16, 17). For example, varicella-zoster virus commonly grows at very low titers but has a very high particle-to-PFU ratio (15). Conversely, bacteriophages have a ratio that is much closer to 1, meaning that all or almost all particles are infectious (18). For filoviruses, there are inconsistencies in the literature; reports have suggested that filoviruses have particle/PFU ratios between 30 (19) and 10,000 (20). Information about the particle/PFU ratio could be useful during outbreak situations when accurate viral detection and quantification are critical.

It has been long recognized that passage of virus results in accumulation of genetic changes as the virus adapts to the cultured cells (18, 21–23). Another well-recognized consequence of passage of viruses is a change in the particle/PFU ratio (24). Here, we tested the consequence of serial EBOV passages for particle/PFU ratio and determined if particle/PFU ratio had an effect on virulence in the cynomolgus macaque model of EBOV infection (EVD).

MATERIALS AND METHODS

Ethics statement. Animal research was conducted under a Texas Biomedical Research Institute (TBRI) Institutional Animal Care and Use Committee (IACUC)-approved protocol (protocol 1381) in compliance with the Animal Welfare Act and other federal statutes and regulations relating to animals and experiments involving animals. The facility where this research was conducted is accredited by the Association for Assessment and Accreditation of Laboratory Animal Care International and adheres to principles stated in the *Guide for the Care and Use of Laboratory Animals* (25). Animals were singly housed and fed monkey biscuits. Enrichment included visual stimulation and commercial toys. Ebola virus exposure occurred on study day 0. Test subjects were then observed at least twice daily for up to 21 days postexposure, at which time the survivors were euthanized for tissue collection. During blood collection, animals were anesthetized using Telazol, and euthanasia criteria were developed to minimize undue pain and distress. Animals were euthanized with an intravenous overdose of sodium pentobarbital. Clinical scores for the animals were reported to the responsible veterinarian, and euthanasia was approved when scores indicated that an animal was terminally ill. Additional euthanasia criteria included a combination of severe petechia or bleeding from any orifice, complete anorexia for 24 h, temperature change of greater than 5°F from baseline, moderate to severe depression (determined by evaluating responsiveness), respiratory distress, thrombocytopenia, or severe elevation of gamma-glutamyltransferase, alanine transaminase, alkaline phosphatase, or blood urea nitrogen.

Cells and virus. BEI-sourced Vero E6 cells (Vero C1008, catalog number NR-596; BEI Resources) were grown in minimum essential medium (MEM; Gibco) containing 2 mM L-glutamine and 1 mM sodium pyruvate (henceforth referred to as normal growth medium) with 10% heat-inactivated fetal calf serum (FCS) (Gibco) at 37°C with 5% CO_2. The starting material for the *in vitro* Vero E6 cell culture passage experiments (results shown in Fig. 1) consisted of: Ebola virus *Homo sapiens*-tc/COD/1995/Kikwit-9510621 (species *Zaire ebolavirus*), passage 2 on Vero E6 cells, acquired from T. Ksiazek, University of Texas Medical Branch. Virus was amplified using the following methods. Vero E6 cells were infected at a multiplicity of infection (MOI) of 0.001 in normal growth medium containing 2% FCS in T75 flasks. Viral supernatant was harvested and clarified by low-speed centrifugation when the cells exhibited 3+ cytopathic effects. Virus was aliquoted and stored in the vapor phase of liquid nitrogen in a cryotank for future use. For the nonhuman primate (NHP) infection studies, the low-particle/PFU-ratio stock (passage 3) was obtained from the U.S. Army Medical Research Institute of Infectious Diseases (USAMRIID). The high-particle/PFU-ratio stock (passage 4) was generated following a single passage of the low-particle/PFU-ratio stock in Vero

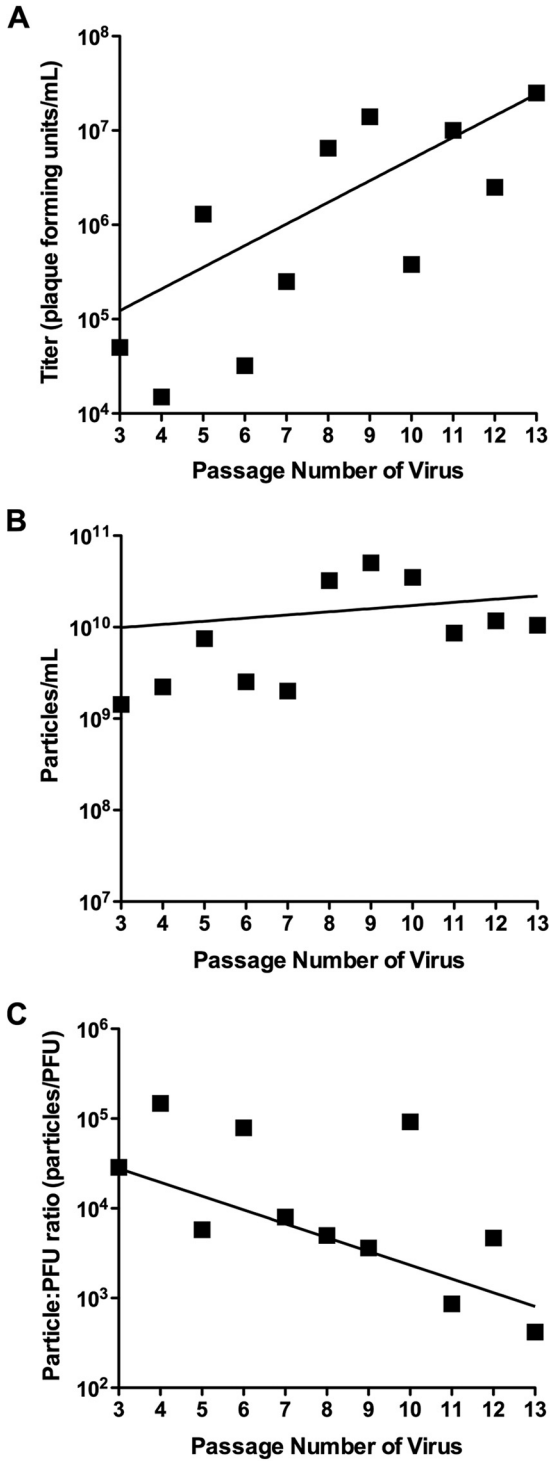

FIG 1 Changes in titer, particle number, and particle/PFU ratio of EBOV passaged in Vero E6 cells. Passage 2 EBOV was serially passaged 10 times in Vero E6 cells at an MOI of 0.001. Lines represent nonlinear regression semilog lines. (A) After each passage, the viral titer (PFU per milliliter) was determined using a plaque assay. (B) After each passage, the number of virus particles per milliliter was determined using electron microscopy. (C) After each passage, the particle/PFU ratio was then determined based on the titer and number of particles.

E6 cells at a low MOI. The two stocks had identical consensus sequences; compared to GenBank accession number AY354458; the only difference was a C (reference) to U (called) at reference position 7327. Both viruses possessed the 8U genotype at the editing site locus (26); the low-particle/PFU-ratio stock was 77% 8U, and the high-particle/PFU-ratio stock was 94% 8U.

Viral passage. Virus was serially passaged 10 times in Vero E6 cells. The initial amplification was performed as described above. After each round of amplification, the viral titer (PFU per milliliter) and viral particle number (particles per milliliter) were determined. After titration, a portion of the virus was used for a subsequent round of amplification.

Determination of viral titers. Viral titers were determined by plaque assay using either a methylcellulose and crystal violet assay or an agarose and neutral red assay (previously described in reference 27). The methylcellulose and crystal violet assay was used to determine the titer of the doses used to infect NHPs, while the agarose and neutral red assay was used for all other viral titrations. Briefly, Vero E6 cells were seeded in 6-well tissue culture plates in either the previously described normal growth medium (agarose assay) or high-glucose Dulbecco's modified Eagle's medium (DMEM) (Gibco) with 10% heat-inactivated FCS and 1% penicillin–streptomycin–L-glutamine (Lonza) (methylcellulose assay). Cells were seeded at a density of 9×10^5 cells per well for the agarose assay and 3×10^5 cells per well for the methylcellulose assay. Inside the animal biosafety level 4 (ABSL4) laboratory, serial 10-fold dilutions of virus were prepared in either normal growth medium containing 2% FCS (agarose assay) or 1× phosphate-buffered saline (PBS) (Gibco) (methylcellulose assay). Medium was decanted from the plates, and 400 μl of each dilution was added to the corresponding well. The plates were incubated for 1 h at 37°C with 5% CO_2, with constant rocking. After incubation, medium was removed from the wells and the primary overlays were added. For the agarose assay, the primary overlay consisted of 1% SeaKem agarose (Lonza) mixed 1:1 with 2× Eagle's minimum essential medium (EMEM) (Lonza) containing 4 mM L-glutamine, 2 mM sodium pyruvate, and 4% FCS (final agarose concentration was 0.5%). A total of 2 ml was added to each well. For the methylcellulose assay, the overlay consisted of high-glucose DMEM (Invitrogen) with 2% heat-inactivated FCS, 1% penicillin–streptomycin–L-glutamine (Lonza), and 16% methylcellulose (Sigma-Aldrich). A total of 5 ml was added to each well. Cells were then incubated at 37°C with 5% CO_2 for the number of days required by each assay. For the agarose assay, on day 7, 2 ml of secondary overlay was added to each well. The secondary overlay consisted of 1% SeaKem agarose (Lonza) mixed 1:1 with 2× EMEM (Lonza) containing 4 mM L-glutamine, 2 mM sodium pyruvate, and 4% FCS (final agarose concentration was 0.5%). Neutral red solution was also added to the secondary overlay at a final concentration of 4%. After the overlay solidified, cells were again incubated at 37°C with 5% CO_2. The following day (8 days postinfection), plates were inspected for plaques, which present as clearings that are visible to the naked eye. Plates were scanned, and plaques were counted to determine a final titer. For the methylcellulose assay, the overlay was removed after 10 days and 5 ml 10% neutral buffered formalin was added to each well to fix the cells. After fixation, formalin was removed and the plates were washed in 1× PBS (Gibco). To stain the plates, 1 ml of crystal violet stain (Ricca Chemical Company) was added to each well and plates were incubated at room temperature for 10 min. The plates were then washed in fresh water and allowed to air dry before plaques were counted with a microscope to determine a final titer.

EM. The electron microscopy (EM) studies were performed using a JEOL 100CX transmission electron microscope. Transmission electron microscopy (TEM) grid preparation was carried out in the ABSL4 laboratory. Viral supernatant from the serially passaged viruses was combined with an equal volume of polystyrene bead suspensions (Duke Standards 3K/4K series particle counter standards). The virus-bead mixtures were then deposited directly onto carbon-Formvar-coated 300-mesh grids and allowed to dry before fixation with 2% glutaraldehyde for 20 min. Next, grids were rinsed with distilled water (dH_2O) and sterilized via exposure to 1% osmium tetroxide fumes for 1 h before being transferred to the BSL2 laboratory. Under a chemical fume hood, grids were removed from the osmium tetroxide and rinsed again with dH_2O. Finally, grids were negatively stained with 1% uranyl acetate. During examination, the edges of 10 random grid squares were imaged, and all viral particles and beads were counted. Since the viral supernatant was mixed 1:1 with polystyrene beads of a known concentration, the following equation was used to determine the particle count: (polystyrene beads counted)/(1×10^9 beads per milliliter) = (viral particles counted)/(actual number of viral particles present per milliliter). The number of viral particles present per milliliter was divided by the number of PFU per milliliter to yield the particle/PFU ratio.

Experimental inoculation of cynomolgus macaques with EBOV. Twelve animals were intramuscularly (i.m.) injected in the deltoid muscle with one of three different doses of EBOV stock that had a low particle/PFU ratio: 0.01 PFU ($n = 4$), 1 PFU ($n = 4$), and 100 PFU ($n = 4$). Twenty animals received three different doses of EBOV stock that had a high particle/PFU ratio: 0.01 PFU ($n = 8$), 1 PFU ($n = 4$), and 100 PFU ($n = 8$). Thirty-two male cynomolgus macaques (*Macaca fascicularis*), 2 to 4 years of age, <4 kg in weight, were used. Animals were acquired from Covance (Covance obtained the animals from an exporter in Vietnam) and serum tested to ensure no reactivity to filovirus antigen prior to purchase. Animals were shipped directly to TBRI for a standard quarantine period. This quarantine period allowed for the animals' health status to be evaluated and allowed time for the animals to acclimate to caging and diet. Ebola virus exposure occurred on study day 0. Test subjects were then observed at least twice daily for up to 21 days postexposure, at which time the survivors were euthanized for tissue collection. Blood samples were collected on days 0, 3, 5, 7, and 14 relative to inoculation for analysis of serology, hematology, clinical chemistry, coagulation parameters, and viral load determination. During each scheduled blood collection, rectal temperature was taken and weight was recorded. When moribund, or at 21 days postinoculation, animals were euthanized with an intravenous overdose of sodium pentobarbital. Necropsy was performed, and gross pathological findings were noted. Samples of liver, spleen, heart, kidney, skin, intestine, lymph node, adrenal gland, lungs, and any gross lesions were aseptically removed and divided (with the exception of lymph nodes, which remained intact) for viral load determination or fixed in 10% neutral phosphate-buffered (pH 7.2) formalin, processed routinely, embedded in paraffin, sectioned at 5 μm, stained with hematoxylin and eosin, and analyzed.

Determination of viral genome copies. Quantitative reverse transcription-PCR (RT-PCR) was used to determine the number of viral genomes present in each of the doses administered to expose the NHPs in this study. An aliquot of each dose was diluted in TRIzol LS reagent (Life Technologies) immediately after inoculum preparation and transferred to the BSL2 laboratory where RNA was harvested according to the manufacturer's instructions. Quantitative RT-PCR was performed as previously described (28) using primers and probe specifically designed to detect a region of the glycoprotein gene. The assay was run on an Applied Biosystems 7500 real-time PCR instrument using the following cycling conditions: 50°C for 15 min (1 cycle), 95°C for 5 min (1 cycle), 95°C for 1 s and 60°C for 35 s (45 cycles), and 40°C for 60 s (1 cycle). A single fluorescence read was taken at the end of each 60°C step.

Statistics. The log-rank Mantel-Cox test was used to analyze the survival curves, and the *P* value is displayed on each graph.

RESULTS

Effects of cell culture passage on EBOV specific infectivity. To determine if specific infectivity is affected by serial passage in cell culture, we performed 10 serial passages of EBOV. The starting material was passage 2 EBOV, and passages were performed at a multiplicity of infection (MOI) of 0.001 (Fig. 1). After each passage, the viral titer (PFU per milliliter) was determined using a plaque assay and the number of virus particles per milliliter was

TABLE 1 Summary of EBOV low- and high-particle/PFU-ratio infection

No. of animals	Dose administered (PFU)	Particle/ PFU ratio	Survival %	Median survival (no. of days)
4	0.01	Low	100	Undefined
4	1.0	Low	0	9
4	100	Low	0	7
8	0.01	High	0	9
4	1.0	High	0	7
8	100	High	0	6

determined using transmission electron microscopy. These two values were then used to calculate the particle/PFU ratio of each passage. As shown in Fig. 1, low-passage-number EBOV stocks cultured in Vero E6 cells yielded high concentrations of particles (1×10^9 to 1×10^{10} particles/ml). The titers were about 10^4-fold lower (1×10^5 or 1×10^6 PFU/ml) than the particle numbers, resulting in a particle/PFU ratio of approximately 1×10^4 particles/PFU. As the virus was passaged, we observed an increase in the concentration of Vero E6-cell-infectious virus particles while the concentration of total particles in the supernatant remained relatively constant. At the highest passage (passage 13), the particle/PFU ratio was approximately 100-fold lower than that for the earliest passages (Fig. 1). Thus, serial passage in Vero E6 cells correlated with a decrease in particle/PFU ratio.

Effects of EBOV specific infectivity during *in vivo* infection. To test the hypothesis that EBOV stocks with high particle/PFU ratios have increased potency relative to stocks with lower particle/PFU ratios, the virulence of two virus stocks was determined using the cynomolgus macaque model of EBOV infection (Table 1). Cynomolgus macaques were exposed intramuscularly to one of three different doses of EBOV stock that had a low particle/PFU ratio, 0.01 PFU ($n = 4$), 1 PFU ($n = 4$), and 100 PFU ($n = 4$), or three different doses of EBOV stock that had a high particle/PFU ratio, 0.01 PFU ($n = 8$), 1 PFU ($n = 4$), and 100 PFU ($n = 8$). The low-particle/PFU-ratio stock had a titer of 4.00×10^6 PFU/ml and contained 2.05×10^9 particles/ml for a final particle/PFU ratio of 5.11×10^2. The high-particle/PFU-ratio stock had a titer of 1.25×10^6 PFU/ml and contained 1.05×10^{10} particles/ml for a final particle/PFU ratio of 8.40×10^3. Importantly, to minimize the number of variables being tested, the two stocks did not differ at the consensus sequence level based on ultradeep sequencing performed using RNA samples from both stocks. After each dose was prepared for the NHP exposure, the concentration of Vero E6-cell-infectious particles present was determined using a plaque assay. The low-particle/PFU dose was determined to contain 89 PFU (performed in duplicate), and the high-particle/PFU dose was determined to contain 153 PFU (performed in quadruplicate). The lowest dose (0.01 PFU) did not contain sufficient Vero E6-cell-infectious particles to accurately quantify using a plaque assay. Thus, quantitative PCR was used to determine the number of viral genomes present in each of the doses. The assay had a limit of detection of 240 genome equivalents. The high-particle/PFU 0.01-PFU dose, which was 100% lethal to the animals, was below this limit of detection. For the low-particle/PFU exposure, the 100-PFU dose was determined to contain 2.7×10^4-fold more genome equivalents than the 0.01-PFU dose.

Blood samples were collected on days 0, 3, 5, 7, and 14. In the low-particle/PFU-ratio infection, the lowest dose (0.01 PFU) did not result in detectable serum titers (Fig. 2). In contrast, animals receiving 1 and 100 PFU of low-particle/PFU virus, or any dose of the high-particle/PFU virus, had high viral titers (measured by plaque assay) in the serum. In general, the higher the dose that an animal received, the earlier that virus was detected in the serum. While a few of the animals receiving 1 PFU of the low-particle/PFU-ratio virus had lower titers than the high-particle/PFU group, the animals receiving the 100-PFU dose all showed similar viral titers in the serum.

Rectal temperature and weight were recorded on days 0, 3, 5, 7, and 14 postexposure (Fig. 3). Animals receiving only 0.01 PFU of both viruses initially exhibited similar weight changes. In the period following expiration of the high-particle/PFU-ratio group, the low-particle/PFU-ratio virus group exhibited minor weight gain. The animals exposed to the high-particle/PFU-ratio virus developed increased temperatures as the study progressed, with many experiencing decreases or return to baseline concurrently with the need for euthanasia. In animals that received 1 PFU of low-particle/PFU-ratio virus, weight remained steady or increased slightly, while this dose of high-particle/PFU-ratio virus correlated with a decrease in weight. Exposure to both viruses resulted in similar increases in temperature for the 1- and 100-PFU groups.

When moribund, or at 21 days postexposure, animals were euthanized and necropsied, and tissues were collected for histology. In animals receiving any dose of the high-particle/PFU virus, the majority exhibited petechial cutaneous rash (18 out of 20) and half exhibited pale liver and/or spleen (10 out of 20). Animals receiving 1 or 100 PFU of low-particle/PFU virus also exhibited petechial cutaneous rash (7 out of 8), though pale liver and/or spleen was less common (1 out of 8). However, animals that received 0.01 PFU of low-particle/PFU virus did not exhibit any petechial cutaneous rash or pale liver and/or spleen. Animals receiving any dose of the high-particle/PFU virus and those receiving 1 or 100 PFU of low-particle/PFU virus also had lesions consistent with Ebola virus-induced hemorrhagic fever (29–31). Histologically significant lesions present in animals that succumbed to acute EBOV infection included lymphoid depletion and necrosis within spleen and lymph nodes, splenic fibrin deposition, and piecemeal hepatocellular necrosis. However, in animals that received the lowest dose of the low-particle/PFU-ratio virus, there was no noticeable pathology in the liver, lymph node, and spleen.

Animals were observed at least twice daily, and clinical scores were recorded (Fig. 4). Of the animals exposed to the low-particle/PFU-ratio virus, those infected with 0.01 PFU exhibited negligible signs of infection, contrasting with animals that received 1 and 100 PFU, which all exhibited severe signs of infection. For the animals exposed to 1 PFU of low-particle/PFU-ratio virus, there was a slight delay in onset of symptoms compared with animals receiving 1 PFU of high-particle/PFU-ratio virus. The particle/PFU ratio did not seem to affect the course of infection in animals receiving 100 PFU of either virus.

Of most relevance, the combination of dose and particle/PFU ratio affected lethality (Fig. 4; Table 1). There was no significant difference in the mean survival times for animals exposed to 100 PFU of either high- or low-particle/PFU virus. However, animals exposed to 1 PFU of the low-particle/PFU virus had a statistically significant longer mean survival time (9 days) than those exposed to 1 PFU of high-particle/PFU virus (7 days). The most dramatic

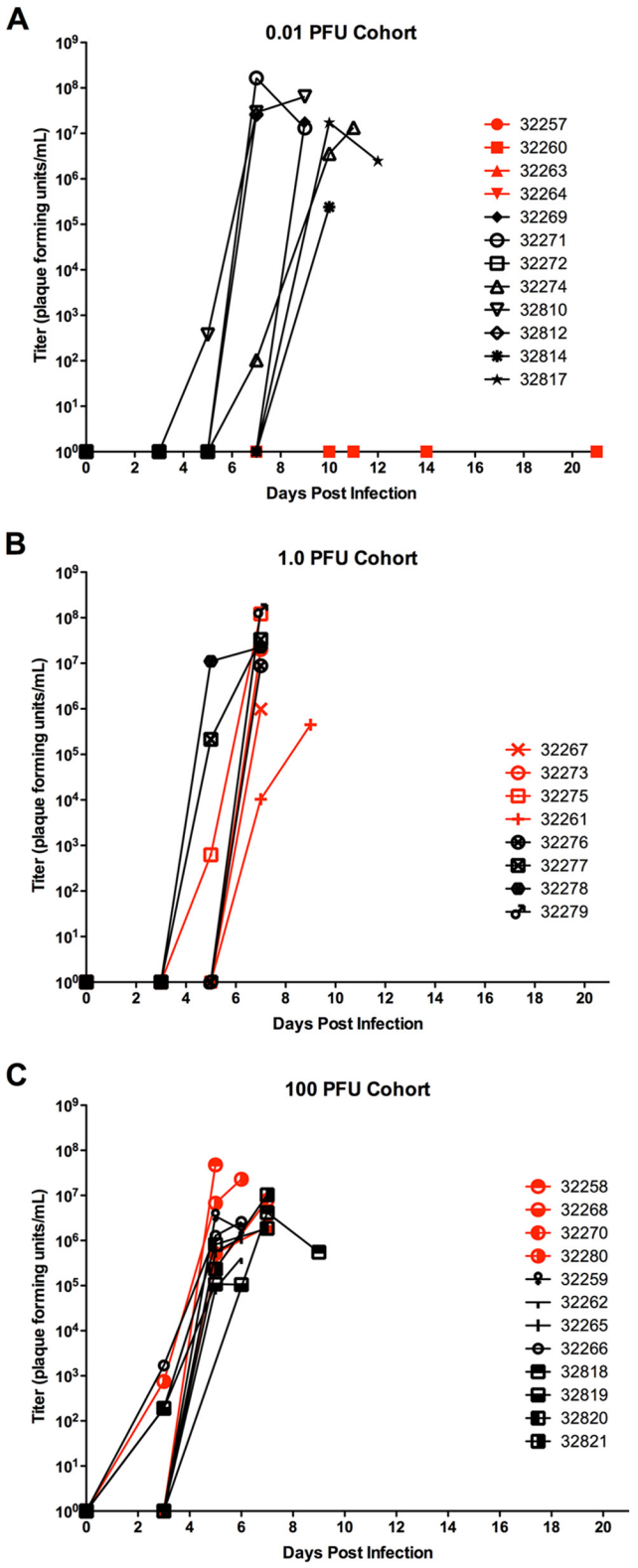

FIG 2 Serum titers from NHPs exposed to low- and high-particle/PFU-ratio EBOV. Animals were observed at least twice daily for up to 21 days postexposure, and blood samples were collected on days 0, 3, 5, 7, and 14 for viral load determination. Red lines and symbols represent animals that received low-particle/PFU-ratio virus. The limit of detection for this assay was 25 PFU/ml. Blood serum titers for animals receiving 0.01 (A), 1 (B), and 100 (C) PFU.

differences in lethality were observed in the group receiving only 0.01 PFU. All animals exposed to 0.01 PFU of the high-particle/PFU virus succumbed to viral infection (mean times of survival were 10 days). In contrast, all animals exposed to 0.01 PFU of the low-particle/PFU virus survived the duration of the study. Moreover, these animals appeared to lack signs of EBOV infection.

DISCUSSION

Ebola virus causes highly lethal hemorrhagic fever, and there are no approved vaccines or therapies to combat the disease. As testing the efficacy of new countermeasures using humans is not ethical, this development requires excellent and well-understood animal models. This includes having a thorough understanding of the properties of the virus used during animal studies. Obvious properties to consider include genome sequence and cell culture titer. However, in most mammalian virus cell culture systems, there are virus particles that are incapable of completing a full infectious cycle or are unable to cause cell pathology in cultured cells. These particles—sometimes referred to as defective particles—are typically ignored. We hypothesized that there are filovirus particles that are incapable of yielding a plaque in cultured Vero E6 cells that can still cause disease in cynomolgus macaques. First, we investigated if passages of EBOV in cell culture influenced specific infectivity. Second, we investigated if specific infectivity influenced EBOV potency and thus virulence in a cynomolgus macaque model of EBOV infection.

The results of the present study suggest that amplification and determination of virus infectivity in the most commonly used EBOV cell culture system (Vero E6 cells, isolated from kidney epithelia of the African green monkey) (27) have undesirable effects that manifest during *in vivo* experiments. Results of the *in vitro* experiments showed that as EBOV was serially passaged, it appeared to be adapting to Vero E6 cell culture. Specifically, there was an increase in the concentration of Vero E6-cell-infectious virus particles following passage despite no great change in the overall concentration of particles. Thus, EBOV passage in Vero E6 cells was associated with a decrease in the particle/PFU ratio. Further work is required to determine if the changes are a consequence of passages of a human virus in a nonhuman cell line.

Having established that different stocks of EBOV may have highly variable specific infectivities, we sought to determine if this was an important consideration in an animal model of EBOV infection. For studies in small-animal models (e.g., mouse or guinea pig), EBOV must be animal adapted in order to cause lethal disease, thus making these animals inappropriate for use in this study (32). Furthermore, this work aimed to ascertain the effect of Vero E6 cell adaptation and specific infectivity during the nonhuman primate studies that are crucial for disease modeling and countermeasure development. Consequently, cynomolgus macaques—the gold standard model for vaccine efficacy studies—were chosen for the animal studies. Animals were exposed to one of two stocks: one stock had a particle/PFU ratio of 8,400, and the other stock had a particle/PFU ratio of 511. All animals exposed to 1 and 100 PFU succumbed to infection. However, at the 0.01-PFU dose, all eight animals exposed to the high-particle-count virus succumbed to infection, while none of the four animals exposed to the low-particle-count virus succumbed to infection. This implies that the high-particle-count virus stock contained virus particles that were able to cause lethal disease in NHPs but were not able to generate plaques in Vero E6 cells (Fig. 5). Conversely, the low-

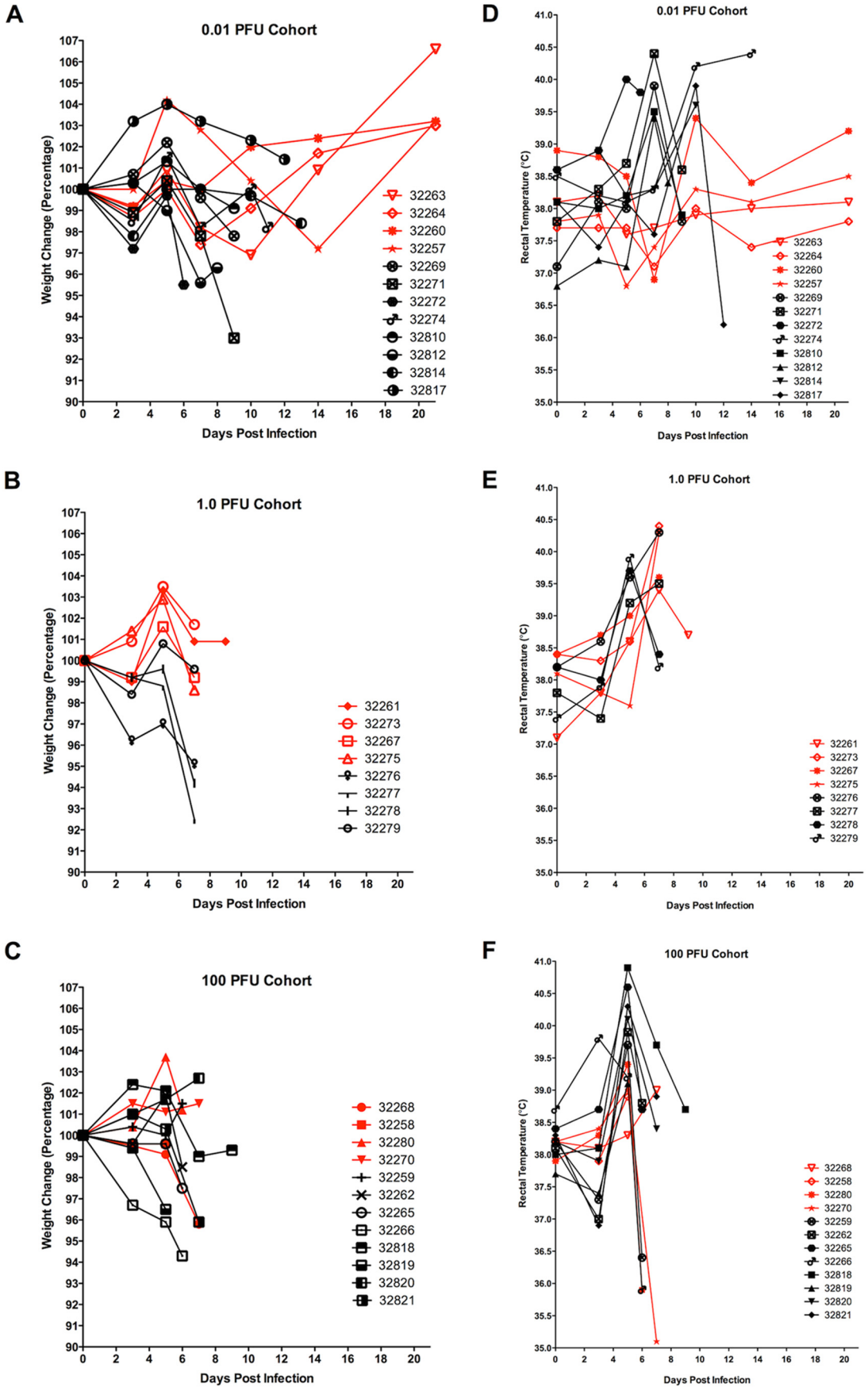

FIG 3 Weight and temperature measurements from NHPs exposed to low- and high-particle/PFU-ratio EBOV. At each scheduled blood collection in the morning, rectal temperature was taken and weight was recorded. Red lines and symbols represent animals that received low-particle/PFU-ratio virus. (A to C) Weight for animals receiving 0.01 (A), 1 (B), or 100 (C) PFU. (D to F) Temperature for animals receiving 0.01 (D), 1 (E), or 100 (F) PFU.

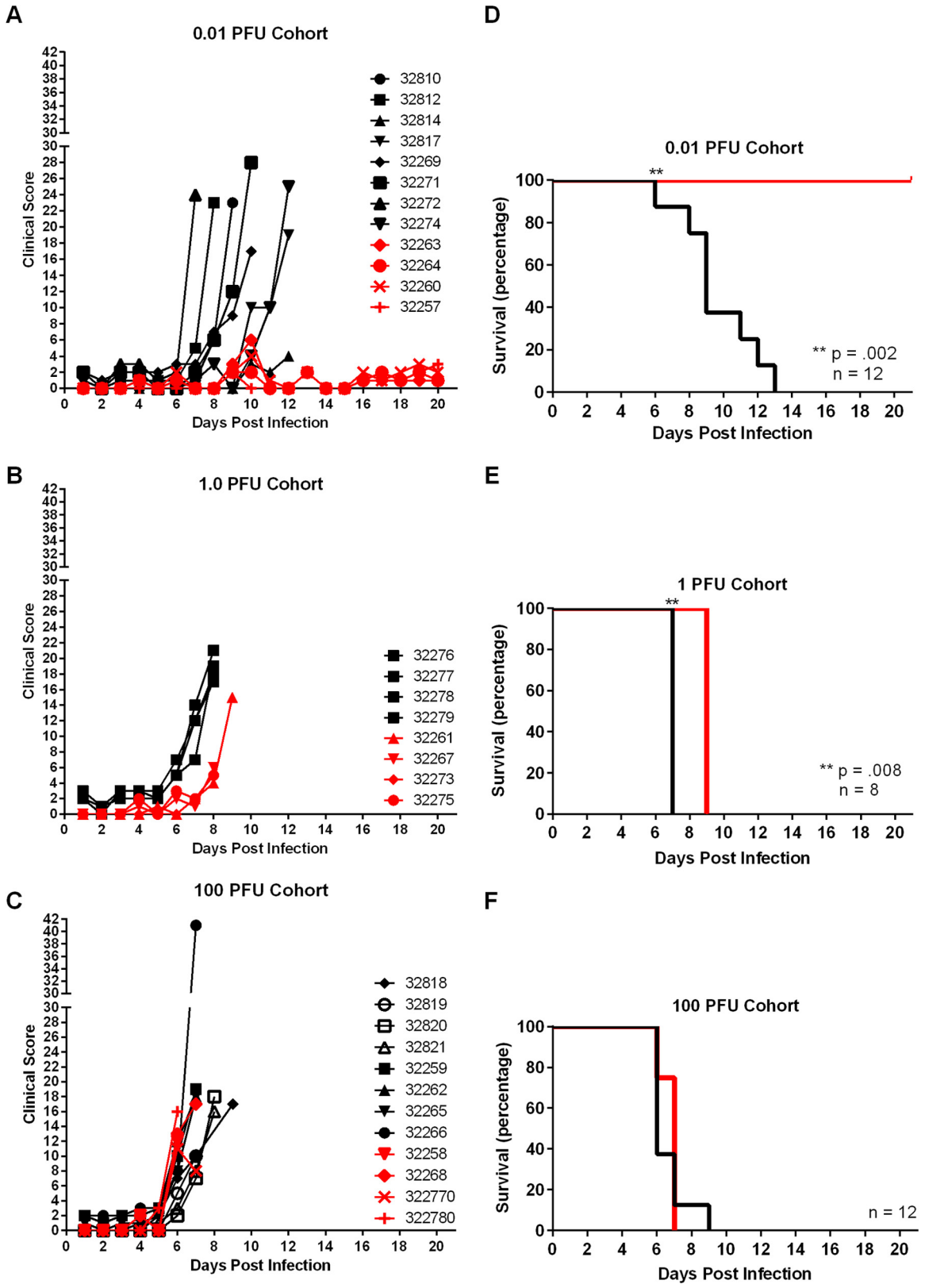

FIG 4 Clinical scores and survival of NHPs exposed to either low- or high-particle/PFU-ratio EBOV. Animals were observed at least twice daily until euthanasia or for up to 21 days, and clinical scores were recorded. Red lines and symbols represent animals that received low-particle/PFU-ratio virus. (A to C) Clinical scores for animals receiving 0.01 (A), 1 (B), or 100 (C) PFU. (D to F) Survival of animals receiving 0.01 (D), 1 (E), or 100 (F) PFU.

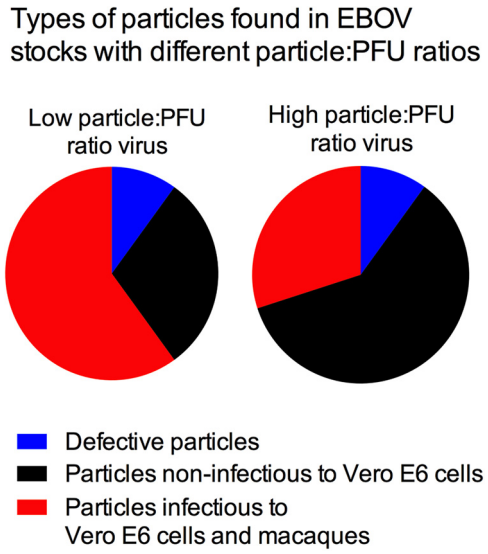

FIG 5 Hypothesized composition of EBOV stocks with different particle/PFU ratios. The data presented in this work suggest that a high-particle/PFU-ratio stock is more potent in cynomolgus macaques than Vero E6 cell culture. We hypothesize that in this stock a larger proportion of the particles are infectious in only cynomolgus macaques, rather than infectious in both cynomolgus macaques and Vero E6 cells. Conversely, the low-particle/PFU-ratio stock may have a lower percentage of particles that are infectious in only cynomolgus macaques as a higher percentage are able to infect both Vero E6 cells and cynomolgus macaques.

particle-count stock did not contain a sufficiently high number of these particles to cause disease in NHPs. The factors responsible for the different phenotypes are likely complex, especially considering that these viruses have identical consensus genome sequences.

It is possible that the particles capable of causing lethal disease in cynomolgus macaques despite not being quantifiable in a Vero E6 cell plaque assay are defective interfering particles (DIs). Defective interfering particles have incomplete coding capacity because of deletions in their genomes. These particles thus rely on other particles containing full-length "helper" genomes to complete a full infectious cycle. The smaller genome size can confer a replicative advantage over full-length helper virions. While defective interfering filovirus particles have been observed *in vitro* (33), without further analysis it is not possible to determine if that classification is appropriate for the particles described in this study.

It is also possible that *in vitro* and *in vivo* infections favor different morphological forms of the virus. Filoviruses are pleomorphic and occur as a mixture that includes filaments of various sizes, tori, commas, and shepherd's crooks, and it is thought that morphology plays a role in virus pathogenicity (34). For example, long filaments may be unable to infect Vero E6 cells *in vitro* but can infect cells important for *in vivo* infection, like macrophages (35). Alternatively, it is possible that *in vitro* the particles clump together, leading several particles to generate only 1 PFU in a plaque assay, while the same clump of particles could separate during *in vivo* infection to yield multiple infectious particles. However, only minimal clumping was observed following EM analyses in both stocks used during the NHP studies. Clearly, further work is required to understand how and why the different preparations of virus have different outcomes *in vivo*.

That 0.01 PFU of Vero E6 cell quantified virus can yield a 100% lethal infection of cynomolgus macaques demonstrates discordance between the plaque assay and infectious dose. Accurate determination of the lethal dose for EBOV appears to be complicated by the effect of the different particle/PFU ratios of various stocks used during *in vivo* studies. Furthermore, our results demonstrate that the amount of high-particle/PFU virus needed to induce disease and mortality in animals may be very small. Consequently, there is a need for an *in vitro* method to quantify EBOV that correlates with *in vivo* potency. Quantitative PCR can be used to measure the number of genomes that are present in a sample. However, its value for filoviruses is limited as filoviruses are polyploid; this means that a single virus particle may contain multiple genomes (36). Further, it is possible to inactivate enveloped virions while maintaining some degree of genome integrity (e.g., with protease). Measurements of numbers of particles are also possible, but this has limitations, which are described elsewhere in this work. These issues are particularly relevant during an outbreak situation where virus detection generally relies on PCR, but there has been a push for the use of methods that can accurately quantify levels of infectious virus (13). Ultimately, the titration of each virus stock in the relevant animal model will yield the most accurate and precise *in vivo* infectivity data, but this has important ethical and financial limitations. Thus, an *in vitro* method that more faithfully recapitulates viral potency in an animal model is required. To this end, we are actively investigating alternative cell culture systems, which are anticipated to be a crucial component of a well-characterized animal model system appropriate for submission to the FDA under the "Animal Rule."

ACKNOWLEDGMENTS

This work was supported by the Department of Defense Medical Countermeasure Systems—Joint Vaccine Acquisition Program (W911QY-12-C-0076). This work was conducted in facilities constructed with support from the Research Facilities Improvement Program (grant number C06 RR012087) from the NCRR.

We thank Marc Mattix for his help compiling the pathology data, Gabriella Worwa and Rebecca Kurnat for helpful comments, the SNPRC veterinary group for outstanding veterinary assistance, and Barbara Hunter at the University of Texas Health Science Center San Antonio Pathology Electron Microscopy Facility for her assistance with the electron microscope. Peter Jahrling and Lisa Hensley kindly provided the low-passage-number material while they were working at USAMRIID, and Thomas Ksiazek at the University of Texas Medical Branch kindly provided the P2 virus. The World Reference Center for Emerging Viruses and Arboviruses contributed to acquisition of the P2 material.

This work is currently being conducted under contract W911QY-12-C-0076 with the U.S. Department of Defense (DoD) Joint Project Manager Medical Countermeasure Systems (JPM-MCS). The views expressed here are those of the authors and do not necessarily represent the views or official position of the DoD or JPM-MCS.

REFERENCES

1. **WHO Ebola Response Team.** 2014. Ebola virus disease in West Africa—the first 9 months of the epidemic and forward projections. N Engl J Med **371:**1481–1495. http://dx.doi.org/10.1056/NEJMoa1411100.
2. **Swanepoel R, Leman PA, Burt FJ, Zachariades NA, Braack LE, Ksiazek TG, Rollin PE, Zaki SR, Peters CJ.** 1996. Experimental inoculation of plants and animals with Ebola virus. Emerg Infect Dis **2:**321–325. http://dx.doi.org/10.3201/eid0204.960407.
3. **Marsh GA, Haining J, Robinson R, Foord A, Yamada M, Barr JA, Payne J, White J, Yu M, Bingham J, Rollin PE, Nichol ST, Wang L-F, Middleton D.** 2011. Ebola Reston virus infection of pigs: clinical signifi-

cance and transmission potential. J Infect Dis **204:**S804–S809. http://dx.doi.org/10.1093/infdis/jir300.
4. **Miranda MEG, Miranda NLJ.** 2011. Reston ebolavirus in humans and animals in the Philippines: a review. J Infect Dis **204**(Suppl 3)**:**S757–S760. http://dx.doi.org/10.1093/infdis/jir296.
5. **Towner JS, Sealy TK, Khristova ML, Albarino CG, Conlan S, Reeder SA, Quan PL, Lipkin WI, Downing R, Tappero JW, Okware S, Lutwama J, Bakamutumaho B, Kayiwa J, Comer JA, Rollin PE, Ksiazek TG, Nichol ST.** 2008. Newly discovered Ebola virus associated with hemorrhagic fever outbreak in Uganda. PLoS Pathog **4:**e1000212. http://dx.doi.org/10.1371/journal.ppat.1000212.
6. **Martina BEE, Osterhaus ADME.** 2009. "Filoviruses": a real pandemic threat? EMBO Mol Med **1:**10–18. http://dx.doi.org/10.1002/emmm.200900005.
7. **Baize S, Pannetier D, Oestereich L, Rieger T, Koivogui L, Magassouba N, Soropogui B, Sow MS, Keïta S, De Clerck H, Tiffany A, Dominguez G, Loua M, Traoré A, Kolié M, Malano ER, Heleze E, Bocquin A, Mély S, Raoul H, Caro V, Cadar D, Gabriel M, Pahlmann M, Tappe D, Schmidt-Chanasit J, Impouma B, Diallo AK, Formenty P, Van Herp M, Günther S.** 2014. Emergence of Zaire Ebola virus disease in Guinea. N Engl J Med **371:**1418–1425. http://dx.doi.org/10.1056/NEJMoa1404505.
8. **Code of Federal Regulations.** 2014. Title 21. Food and drugs. Chapter I. Food and Drug Administration. Subchapter D. Drugs for human use. Part 314. Applications for FDA approval to market a new drug. Subpart I. Approval of new drugs when human efficacy studies are not ethical or feasible. 21 CFR 314.600.
9. **Code of Federal Regulations.** 2014. Title 21. Food and drugs. Chapter I. Food and Drug Administration. Subchapter F. Biologics. Part 601. Licensing. Subpart H. Approval of biological products when human efficacy studies are not ethical or feasible. 21 CFR 601.90.
10. **Food and Drug Administration.** 2002. New drug and biological drug products; evidence needed to demonstrate effectiveness of new drugs when human efficacy studies are not ethical or feasible. Final rule. Fed Regist **67:**37988–37998.
11. **Gronvall GK, Trent D, Borio L, Brey R, Nagao L.** 2007. The FDA animal efficacy rule and biodefense. Nat Biotechnol **25:**1084–1087. http://dx.doi.org/10.1038/nbt1007-1084.
12. **Sullivan NJ, Martin JE, Graham BS, Nabel GJ.** 2009. Correlates of protective immunity for Ebola vaccines: implications for regulatory approval by the animal rule. Nat Rev Microbiol **7:**393–400. http://dx.doi.org/10.1038/nrmicro2129.
13. **Institute of Medicine National Research Council.** 2014. Research priorities to inform public health and medical practice for Ebola virus disease: workshop in brief. The National Academies Press, Washington, DC.
14. **Schwerdt CE, Fogh J.** 1957. The ratio of physical particles per infectious unit observed for poliomyelitis viruses. Virology **4:**41–52. http://dx.doi.org/10.1016/0042-6822(57)90042-9.
15. **Carpenter JE, Henderson EP, Grose C.** 2009. Enumeration of an extremely high particle-to-PFU ratio for varicella-zoster virus. J Virol **83:**6917–6921. http://dx.doi.org/10.1128/JVI.00081-09.
16. **Frey TK.** 1994. Molecular biology of rubella virus. Adv Virus Res **44:**69–160. http://dx.doi.org/10.1016/S0065-3527(08)60328-0.
17. **Coffey LL, Vignuzzi M.** 2011. Host alternation of Chikungunya virus increases fitness while restricting population diversity and adaptability to novel selective pressures. J Virol **85:**1025–1035. http://dx.doi.org/10.1128/JVI.01918-10.
18. **Luria SE, Anderson TF.** 1942. The identification and characterization of bacteriophages with the electron microscope. Proc Natl Acad Sci U S A **28:**127–130.1. http://dx.doi.org/10.1073/pnas.28.4.127.
19. **Bray M, Davis K, Geisbert T, Schmaljohn C, Huggins J.** 1999. A mouse model for evaluation of prophylaxis and therapy of Ebola hemorrhagic fever. J Infect Dis **179**(Suppl 1)**:**S248–S258. http://dx.doi.org/10.1086/514292.
20. **Weidmann M, Sall A, Manuguerra J-C, Koivogui L, Adjami A, Traore F, Hedlund K-O, Lindegren G, Mirazimi A.** 2011. Quantitative analysis of particles, genomes and infectious particles in supernatants of haemorrhagic fever virus cell cultures. Virology J **8:**81. http://dx.doi.org/10.1186/1743-422X-8-81.
21. **Sobrino F, Dávila M, Ortín J, Domingo E.** 1983. Multiple genetic variants arise in the course of replication of foot-and-mouth disease virus in cell culture. Virology **128:**310–318. http://dx.doi.org/10.1016/0042-6822(83)90258-1.
22. **Domingo E, Escarmís C, Sevilla N, Moya A, Elena SF, Quer J, Novella IS, Holland JJ.** 1996. Basic concepts in RNA virus evolution. FASEB J **10:**859–864.
23. **Holland J, Spindler K, Horodyski F, Grabau E, Nichol S, VandePol S.** 1982. Rapid evolution of RNA genomes. Science **215:**1577–1585. http://dx.doi.org/10.1126/science.7041255.
24. **Thompson K, Yin J.** 2010. Population dynamics of an RNA virus and its defective interfering particles in passage cultures. Virology J **7:**257. http://dx.doi.org/10.1186/1743-422X-7-257.
25. **National Research Council.** 2011. Guide for the care and use of laboratory animals, 8th ed. National Academies Press, Washington, DC.
26. **Kugelman JR, Lee MS, Rossi CA, McCarthy SE, Radoshitzky SR, Dye JM, Hensley LE, Honko A, Kuhn JH, Jahrling PB, Warren TK, Whitehouse CA, Bavari S, Palacios G.** 2012. Ebola virus genome plasticity as a marker of its passaging history: a comparison of in vitro passaging to non-human primate infection. PLoS One **7:**e50316. http://dx.doi.org/10.1371/journal.pone.0050316.
27. **Shurtleff A, Biggins J, Keeney A, Zumbrun E, Bloomfield H, Kuehne A, Audet J, Alfson K, Griffiths A, Olinger G, Bavari S.** 2012. Standardization of the filovirus plaque assay for use in preclinical studies. Viruses **4:**3511–3530. http://dx.doi.org/10.3390/v4123511.
28. **Trombley AR, Wachter L, Garrison J, Buckley-Beason VA, Jahrling J, Hensley LE, Schoepp RJ, Norwood DA, Goba A, Fair JN, Kulesh DA.** 2010. Comprehensive panel of real-time TaqMan polymerase chain reaction assays for detection and absolute quantification of filoviruses, arenaviruses, and New World hantaviruses. Am J Trop Med Hyg **82:**954–960. http://dx.doi.org/10.4269/ajtmh.2010.09-0636.
29. **Chamanza R, Marxfeld HA, Blanco AI, Naylor SW, Bradley AE.** 2010. Incidences and range of spontaneous findings in control cynomolgus monkeys (Macaca fascicularis) used in toxicity studies. Toxicol Pathol **38:**642–657. http://dx.doi.org/10.1177/0192623310368981.
30. **Geisbert TW, Hensley LE, Larsen T, Young HA, Reed DS, Geisbert JB, Scott DP, Kagan E, Jahrling PB, Davis KJ.** 2003. Pathogenesis of Ebola hemorrhagic fever in cynomolgus macaques: evidence that dendritic cells are early and sustained targets of infection. Am J Pathol **163:**2347–2370. http://dx.doi.org/10.1016/S0002-9440(10)63591-2.
31. **Baskerville A, Bowen ET, Platt GS, McArdell LB, Simpson DI.** 1978. The pathology of experimental Ebola virus infection in monkeys. J Pathol **125:**131–138. http://dx.doi.org/10.1002/path.1711250303.
32. **Nakayama E, Saijo M.** 2013. Animal models for Ebola and Marburg virus infections. Front Microbiol **4:**267. http://dx.doi.org/10.3389/fmicb.2013.00267.
33. **Calain P, Monroe MC, Nichol ST.** 1999. Ebola virus defective interfering particles and persistent infection. Virology **262:**114–128. http://dx.doi.org/10.1006/viro.1999.9915.
34. **Booth TF, Rabb MJ, Beniac DR.** 2013. How do filovirus filaments bend without breaking? Trends Microbiol **21:**583–593. http://dx.doi.org/10.1016/j.tim.2013.08.001.
35. **Stroher U, West E, Bugany H, Klenk HD, Schnittler HJ, Feldmann H.** 2001. Infection and activation of monocytes by Marburg and Ebola viruses. J Virol **75:**11025–11033. http://dx.doi.org/10.1128/JVI.75.22.11025-11033.2001.
36. **Beniac DR, Melito PL, Devarennes SL, Hiebert SL, Rabb MJ, Lamboo LL, Jones SM, Booth TF.** 2012. The organisation of Ebola virus reveals a capacity for extensive, modular polyploidy. PLoS One **7:**e29608. http://dx.doi.org/10.1371/journal.pone.0029608.